NANO LETTERS

Letter

pubs.acs.org/NanoLett

Vapor Sensing Characteristics of Nanoelectromechanical Chemical Sensors Functionalized Using Surface-Initiated Polymerization

Heather C. McCaig,[†] Ed Myers,[‡] Nathan S. Lewis,*[,†] and Michael L. Roukes*[,‡]

[†]Kavli Nanoscience Institute and Division of Chemistry and Chemical Engineering, California Institute of Technology, Pasadena, California 91125, United States

[‡]Kavli Nanoscience Institute and Condensed Matter Physics, California Institute of Technology, Pasadena, California 91106, United States

Supporting Information

ABSTRACT: Surface-initiated polymerization has been used to grow thick, uniform poly(methyl methacrylate) films on nanocantilever sensors. Cantilevers with these coatings yielded significantly greater sensitivity relative to bare devices as well as relative to devices that had been coated with drop-cast polymer films. The devices with surface-initiated polymer films also demonstrated high selectivity toward polar analytes. Surface-initiated polymerization can therefore provide a straightforward, reproducible method for large-scale functionalization of nanosensors.

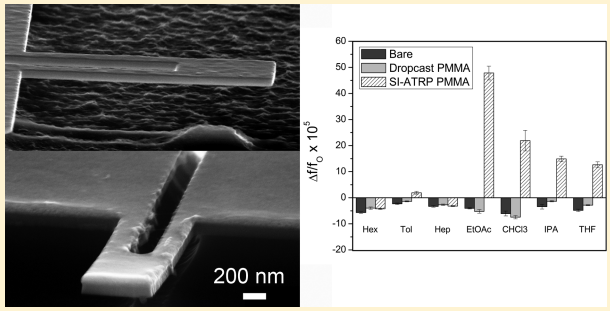

KEYWORDS: *Cantilever sensor, nanocantilever, nanomechanical resonator, chemical vapor sensor, surface-initiated polymerization, ATRP*

Resonant micro- and nanocantilever sensors,[1,2] modified with self-assembled monolayers (SAMs) or polymer films, have been used to detect a variety of biological and chemical species,[3−6] including chemical vapors.[7−11] Sorption of a chemical vapor onto the surface of a cantilever changes factors such as the mass and stiffness of the cantilever, which in turn induces shifts in the resonant frequency of the structure.[2] The analyte sensitivity increases as the size of such resonant structures decreases[12] with nanocantilevers demonstrated to detect mass changes down to the attogram (10^{-18} g) scale in ambient conditions[10] and at and below the zeptogram (10^{-21} g) scale in vacuum.[13−16]

The functionalization of nanocantilevers with polymer films increases the sorption of chemical vapors onto the sensor, relative to the behavior of bare sensors. Functionalization also imparts selectivity to the sensor based on the differences between chemical interactions of various polymer/vapor pairs. In response to chemical vapors under ambient conditions, the signal-to-noise ratio of the sensors increases as the film thickness increases. Previous nanocantilever chemical vapor sensor studies have relied on thin, 2−10 nm drop-cast polymer films,[10,11] which, while effective, limit the sensor's dynamic range in terms of both the minimum and maximum detectable vapor concentrations. Top-down coating techniques, such as microcapillary-pipet-assisted drop-casting[17] and inkjet printing,[18] utilize solvent evaporation to produce solid films. These methods result in films of nonuniform thickness, resulting in a low yield of well-coated sensors, and a high degree of irreproducibility between adjacent sensors. Surface-initiated polymerization (SIP) from a variety of precursors has been widely used to grow polymers directly on the surfaces of devices.[19] The resulting films are composed of polymer chains with one end tethered to a substrate. When the interchain distance is small, steric repulsion leads to chain stretching, resulting in a brushlike conformation. Functionalization of nanocantilevers with SIP-grown films provides a method to deposit sorptive films. Surface-initiated atom-transfer radical polymerization (SI-ATRP) is a particular polymer brush-growth technique that is versatile and easily implemented with a wide range of functional groups.[20] SI-ATRP has been used to grow polymer brushes on microcantilevers that have been subsequently used to detect changes in solvent quality,[21,22] pH,[22] and temperature,[22,23] as well as to detect the presence of glucose in liquids[24] and to detect saturated toluene vapor in nitrogen.[25] These microcantilever-based measurements of changes in gaseous environments were performed with a readout based on the static deflection of the cantilever device of interest.

We describe herein the use of surface-initiated polymerization to grow thick, sorptive films on nanocantilever chemical vapor sensors. Specifically, poly(methyl methacrylate) (PMMA) has been grown directly from the surface of nanocantilevers via SI-ATRP, using a synthetic method that confines the formation of the polymer to the cantilever surface.

Received: February 6, 2014
Revised: June 10, 2014
Published: June 12, 2014

 © 2014 American Chemical Society

The SI-ATRP PMMA-coated cantilevers were then exposed to a series of seven organic vapors, along with both bare cantilevers and cantilevers functionalized with a drop-cast PMMA film. In contrast to using a readout based on the static deflection of the device, dynamic detection based on the resonance frequency shift of the cantilever was utilized as the sensing signal. The SI-ATRP PMMA-coated cantilever response to polar analytes was enhanced relative to bare and drop-cast PMMA-coated cantilevers, while all sensors exhibited mutually similar magnitudes of responses to nonpolar vapors. The thick polymer films grown by SI-ATRP on resonant nanocantilever sensors have enabled new studies in which the sensor responses are dominated by analyte absorption into polymers. Notably, these films are readily adaptable to wafer-scale processing.

The properties of surface-functionalized sensors using SI-ATRP were explored by use of piezoresistive, gold-coated, silicon nitride nanocantilevers[10,26,27] with a typical fundamental resonance frequency of 10−12 MHz, quality factors (Q's) of 100−200 in ambient conditions, and a capture area of 1.5 μm^2. The cantilever resonance was actuated thermoelastically using integrated Joule heating elements in conjunction with an AC drive current.[28] The nanocantilever sensors were controlled with custom, LabView-controlled, electronics[27] that continuously tracked the resonance frequency of each sensor through the use of parallel and independent phase-locked loops (PLLs). For surface polymerization, after a thorough cleaning by a UV/ozone plasma the polymerization initiator bis(2-[2′-bromoisobutyryloxy]ethyl)disulfide (BiBOEDS) (ATRP Solutions) was tethered to a gold overlayer on each cantilever by self-assembly, involving immersion of the substrate in a 5 mM solution of BiBOEDS in C_2H_5OH for 24−36 h. The PMMA polymer brush was then grown using a room-temperature, water-accelerated reaction[29] that was allowed to proceed for between 30 min and 30 h. Additional details on the synthetic procedures are provided in the Supporting Information.

Figure 1 presents ellipsometric measurements of PMMA films grown on flat, gold-coated substrates. These films displayed an initial linear relationship between the reaction time and the film thickness with the relationship deviating from linearity at long times due to chain termination. For reaction times less than 20 h, the standard deviation of the film thickness for a given reaction time was less than 3.5% of the average film thickness. A maximum film thickness of ∼90 nm was reached after 20 h of film growth. For reaction times of >20 h, larger scatter was observed in the final film thickness, likely due to a higher rate of polymer chain termination relative that observed at shorter reaction times. As shown in Figure 2, scanning electron micrograph (SEM) images of a nanocantilever coated with a 90 nm thick SI-ATRP PMMA film indicated that the resulting films were smooth with a uniform thickness across the nanocantilever, which is in contrast to the morphology characteristic of sensors coated with drop-cast PMMA films.

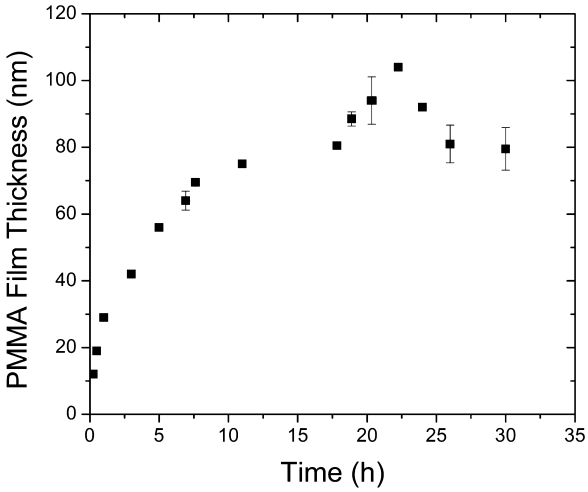

Figure 1. Dependence of the thickness of PMMA films grown by SI-ATRP PMMA on the reaction time. The film reached a maximum film thickness of ∼90 nm after ∼20 h of film growth. For data points representing multiple trials, the error bars indicate the standard deviation of the thickness of the PMMA films grown for a given reaction time.

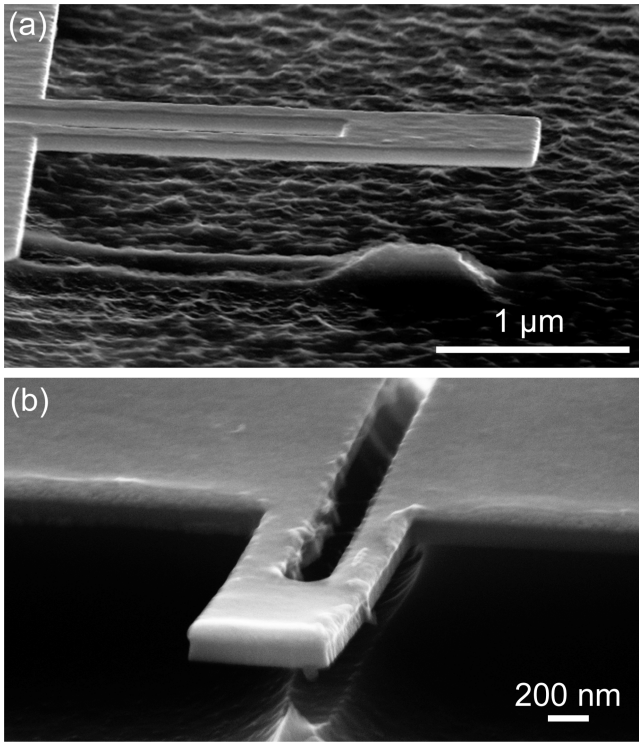

Figure 2. Scanning electron microscope images of nanocantilevers functionalized with (a) a 10 nm thick, dropcast PMMA film and (b) a 90 nm thick, PMMA film grown by SI-ATRP.

Nanocantilevers were exposed to analyte vapors using an automated vapor delivery system controlled by LabView-based software.[30] The analytes (hexane, toluene, heptane, ethyl acetate, chloroform, tetrahydrofuran, and isopropanol) were delivered at concentrations of P/P° = 0.0050−0.080 (where P is the partial pressure and P° is the saturated vapor pressure of the analyte at room temperature). Each exposure consisted of 70 s of pure carrier gas, 400 s of analyte vapor exposure, and 630 s of carrier gas to purge the system. For single concentration experiments, a given run consisted of five exposures to each analyte at P/P° = 0.020. To ascertain the linearity of the functionalized nanocantilever response with respect to analyte concentration, five exposures per concentration, per analyte, were delivered in the order P/P° = 0.030, 0.010, 0.048, 0.0050, 0.080, and 0.020 to minimize potential hysteresis in the measured linearity profiles. SI-ATRP PMMA-coated cantilevers were also exposed to polar vapors for longer

dx.doi.org/10.1021/nl500475b | Nano Lett. 2014, 14, 3728−3732

times, that is, up to as much as 5000 s, to determine both the equilibrium response and the response time of the sensors. Additional details of the measurement protocols are provided in the Supporting Information.

For all vapor exposure experiments, the nanocantilevers were housed in a sealed brass chamber with an internal volume of 100 mL. One to four sensors were tested in each experimental run, and all sensors were "broken-in" prior to data collection by multiple exposures to each analyte. The temperature of the device and chamber were not controlled directly but were stable at 21 °C to within ±1 °C. Frequency data were corrected for any baseline drift prior to extraction of the sensor responses. The baseline noise was computed as the standard deviation of the drift-corrected baseline frequency over a period of 10 s prior to the sensor response. The signal-to-noise ratio (SNR) was calculated as the average response divided by three times the baseline noise.

Figure 3 shows data from analyte exposures of 400 s, indicating that cantilevers coated with the SI-ATRP PMMA film produced larger responses to polar vapors relative both to devices without coatings as well as compared to devices coated with drop-cast PMMA films. However, no signal enhancement was observed for nonpolar vapors. Figure 4 presents the dependence of the sensor response on the vapor concentration for 400 s exposures of vapor to a cantilever-coated with a PMMA film grown by SI-ATRP. The sensor showed a nearly linear response to toluene vapor, but the responses to ethyl acetate and to isopropanol deviated from linearity at high analyte concentrations.

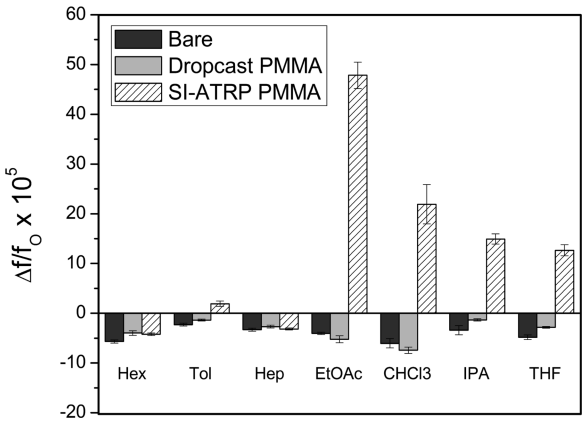

Figure 3. Responses of nanocantilever sensors to a series of 400 s exposures to analyte vapors, delivered at $P/P^{\circ} = 0.02$. Nanocantilevers coated with PMMA films grown by SI-ATRP showed enhanced sensitivity to polar analytes relative to nonpolar analytes.

The enhanced sensitivity to polar analytes and the lack of sensitivity enhancement for nonpolar analytes cannot be readily explained from differences in the respective partition coefficients of analytes into PMMA films grown by SI-ATRP. The partition coefficient (K_{eq}) for an analyte/polymer pair is defined as

$$K_{eq} = \frac{C_f}{C_v} \tag{1}$$

where C_f is the concentration of the analyte in the polymer film and C_v is the concentration of the analyte in the vapor phase.[31] Hence, the number of molecules absorbed into the polymer film is not correlated with the magnitude of the response. The relative mass loading of the polymer film (calculated as the product of the partition coefficient and the molecular weight of the analyte) also does not correlate with response magnitude. (The Supporting Information provides K_{eq} values for both bulk PMMA and SI-ATRP PMMA films for all analytes employed in this study).

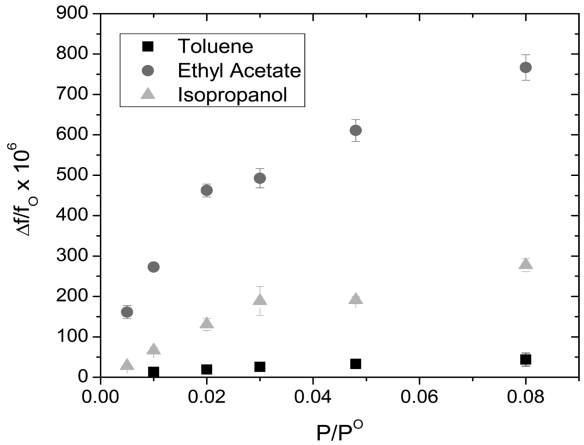

Figure 4. Sensor response versus analyte concentration for cantilevers coated with PMMA films grown using SI-ATRP. Slow diffusion into the PMMA film by ethyl acetate and isopropanol led to a departure from linearity for these two analytes.

The enhanced sensitivity to polar vapors of nanocantilevers that had been coated with PMMA grown by SI-ATRP also cannot be ascribed to vertical swelling of the polymer brush in response to the presence of analyte vapors. The largest relative change in thickness of SI-ATRP PMMA films was observed upon exposure to saturated chloroform vapor. Progressively smaller responses were observed upon exposure to tetrahydrofuran, ethyl acetate, isopropanol, toluene, heptane, and hexane vapors, respectively. The differences in magnitude of the relative thickness changes do not correlate with the observed responses of the functionalized cantilever sensors. Additionally, the ratio of the relative film swelling to the K_{eq} for each vapor was an order of magnitude greater for chloroform and tetrahydrofuran, two good solvents for PMMA,[32] compared to that of the other analyte vapors.

The magnitude of the response of SI-ATRP PMMA-coated nanocantilevers correlates with the dipole moment of the analyte vapors (see Supporting Information). To test the validity of this correlation, cantilevers coated with PMMA grown by SI-ATRP were exposed to carbon tetrachloride, which is chemically similar to chloroform, but that has no dipole moment. As shown in Table 1, a 400 s exposure to chloroform induced a relative frequency shift of 2.19×10^{-4}, whereas a 400 s exposure to carbon tetrachloride caused a relative frequency shift of only -4.11×10^{-5}. This behavior is consistent with expectations in which analytes with nonzero dipole moments interact more strongly with PMMA and induce changes in the polymer film that yield increased sensor stiffness that in turn is manifested as large positive shifts in the resonance frequency of the cantilever. The sensitivity of sorption-based vapor sensors has been shown to correlate primarily with the fractional vapor pressure of the analyte, as opposed to the absolute value of the analyte concentration in the gas phase.[33] For a given concentration (mol/volume) of vapor, analytes with higher vapor pressures (such as those used in this study) experience a lower thermodynamic driving force

dx.doi.org/10.1021/nl500475b | Nano Lett. 2014, 14, 3728−3732

Table 1. Magnitude of the Frequency Shift of a SI-ATRP PMMA Coated Nanocantilever Exposed to 400 s Pulses of Analyte Vapors Correlates with the Dipole Moment of the Analyte[a]

SI-ATRP PMMA nanocantilever frequency shift and analyte dipole moment		
analyte	$\Delta f_{max}/f_O \times 10^6$	dipole moment (D/μ)[b]
hexane	−42.37 ± 2.62	0
toluene	18.94 ± 5.45	0.375 ± 0.010
heptane	−31.67 ± 2.39	0
ethyl acetate	478.36 ± 26.47	1.78 ± 0.09
chloroform	219.21 ± 39.51	1.04 ± 0.02
isopropanol	149.13 ± 10..28	1.58 ± 0.03
tetrahydrofuran	126.52 ± 11.27	1.75 ± 0.04
carbon tetrachloride	−41.13 ± 2.64	0

[a]Analytes with a dipole moment of zero induced small frequency shifts, while analytes with non-zero dipoles induced large, positive frequency shifts. [b]Dipole moment values taken from the CRC Handbook of Chemistry and Physics, 82nd edition.[46]

to absorb into the polymer film than analytes with low vapor pressures (e.g., organophosphate nerve agents and explosives). Therefore, nanocantilevers coated with an appropriate polymer film are expected to be more sensitive to low vapor pressure analytes compared to higher vapor pressure analytes.

These positive shifts in nanocantilever resonance frequency can be represented by the relation

$$\frac{\Delta f}{f_O} = \frac{\delta k}{2k} - \frac{\delta m_{eff}}{2m_{eff}} \quad (2)$$

In eq 2, Δf is the change in frequency, f_O is the fundamental resonance frequency, k is the initial stiffness, δk is the change in stiffness, m_{eff} is the initial effective mass, and δm_{eff} is the change in effective mass.[7] The simple sorption of vapor molecules onto a nanocantilever will result in an increase in mass. If the sorption-induced mass increase is the sole effect, the cantilever should therefore experience a decrease in its resonance frequency. For a positive frequency shift to be observed in response to sorption of an analyte vapor, a concomitant increase in sorption-induced sensor stiffness must occur, and this effect must dominate the effects of mass loading. This phenomenon has been observed in microcantilevers used for gas sensing,[7] as well as for nanocantilevers used to detect chemical vapors[34] and biological species.[35−37] Consistently, the resonance frequency of a microcantilever either increased or decreased after evaporation of a gold film onto the device, depending on whether the gold was deposited at the clamped end or at the free end of the cantilever, respectively.[38] For vapor absorption into glassy PMMA films grown by SI-ATRP, the effects of small molecules interpenetrating the polymer chains could account for the observed increase in sensor stiffness.[2]

Figure 4 shows the response of nanocantilevers coated with PMMA films grown by SI-ATRP over a range of partial pressures of toluene, isopropanol, and ethyl acetate. Such sensors showed a linear response for small toluene partial pressures but showed nonlinear responses during exposure to the same range of partial pressures of ethyl acetate or isopropanol. The shapes of the response data can be explained by the relative diffusion rates of the analytes partitioning into the 90 nm thick PMMA films grown by SI-ATRP. The nanocantilever sensors were operated at ∼30 °C, whereas the glass transition temperature (T_g) of the bulk PMMA (Scientific Polymer Products, Inc.; molecular weight = 35 000) used for the drop-cast films is 105 °C.[39] At temperatures well below T_g, the individual chains of a polymer are locked into a small set of configurations, rendering the polymer "glassy" and decreasing the diffusion rate of vapor molecules into the film relative to the diffusion rate above the same polymer's T_g. Glassy polymers such as PMMA are known to exhibit diffusion of analytes that does not follow Fick's Law. Instead, diffusion involves delayed relaxation of the polymer chains, which can greatly increase the time required for the absorbed analyte to reach its steady-state concentration.[40−43] Specifically, the profiles of the sensor responses were similar to the behavior observed in dual-mode sorption in which the following two populations of sorbed analyte molecules are present: those dissolved within matrix of the polymer chains (described by Henry's Law) and those residing in holes of free volume in polymer film (described by a Langmuir expression).[44,45] The nanocantilever responses did not reach steady state during 400 s exposures to ethyl acetate at any concentration explored. Similar behavior was observed for exposure to isopropanol vapor at concentrations above P/P° = 0.02. The sensors only reached a steady-state response to ethyl acetate after ∼5000 s of exposure.

We therefore have described a method for enhancing the absorption of vapor onto nanocantilevers sensors by deposition of thick, uniform polymer films via the SI-ATRP process. The approach circumvents the limitations of top-down functionalization schemes, such as standard drop-coating techniques, and yields sensors with both improved sensitivity and enhanced saturation limits. The method also enables facile tailoring of the physical and chemical properties of the polymer films for specific sensing applications. Advanced chemical functionalization techniques, such as the surface-initiated polymerization presented here, will accelerate the adoption of miniaturized, nanocantilever-based vapor detection platforms for a wide spectrum of applications.

■ ASSOCIATED CONTENT

Supporting Information

Details of our experimental procedures, tabulated response data, sensor response characteristics, fitting procedures to deduce response times, partition coefficients for the drop-cast and SI-ATRP-grown PMMA films, and further discussion of the results of sensor responses to 5000 s exposures of vapors. This material is available free of charge via the Internet at http://pubs.acs.org.

■ AUTHOR INFORMATION

Corresponding Authors

*E-mail: (N.S.L.) nslewis@caltech.edu.
*E-mail: (M.L.R.) roukes@caltech.edu.

Notes

The authors declare no competing financial interest.

■ ACKNOWLEDGMENTS

We gratefully acknowledge assistance from Derrick Chi in fabrication of the NEMS devices, from Xinchang Zhang for development of the NEMS control electronics, the Caltech Geology and Planetary Science Analytical Facility and the Kavli Nanoscience Institute for SEM imaging, and from Bruce S. Brunschwig and the Molecular Materials Research Center for the use of their ellipsometer. We acknowledge support for this

work from DARPA/MTO-MGA through Grant NBCH1050001, and from the Department of Homeland Security, Centers of Excellence, Agreement 2008-ST-061-ED0002.

REFERENCES

(1) Boisen, A.; Dohn, S.; Keller, S. S.; Schmid, S.; Tenje, M. *Rep. Prog. Phys.* **2011**, *74* (3), 30.
(2) Eom, K.; Park, H. S.; Yoon, D. S.; Kwon, T. *Phys. Rep.* **2011**, *503* (4−5), 115−163.
(3) Lavrik, N. V.; Sepaniak, M. J.; Datskos, P. G. *Rev. Sci. Instrum.* **2004**, *75* (7), 2229−2253.
(4) Singamaneni, S.; LeMieux, M. C.; Lang, H. P.; Gerber, C.; Lam, Y.; Zauscher, S.; Datskos, P. G.; Lavrik, N. V.; Jiang, H.; Naik, R. R.; Bunning, T. J.; Tsukruk, V. V. *Adv. Mater.* **2008**, *20* (4), 653−680.
(5) Zougagh, M.; Rios, A. *Analyst* **2009**, *134* (7), 1274−1290.
(6) Hwang, K. S.; Lee, S. M.; Kim, S. K.; Lee, J. H.; Kim, T. S. *Annu. Rev. Anal. Chem.* **2009**, *2*, 77−98.
(7) Thundat, T.; Chen, G. Y.; Warmack, R. J.; Allison, D. P.; Wachter, E. A. *Anal. Chem.* **1995**, *67* (3), 519−521.
(8) Maute, M.; Raible, S.; Prins, F. E.; Kern, D. P.; Ulmer, H.; Weimar, U.; Gopel, W. *Sens. Actuators, B* **1999**, *58* (1−3), 505−511.
(9) Pinnaduwage, L. A.; Ji, H. F.; Thundat, T. *IEEE Sens. J.* **2005**, *5* (4), 774−785.
(10) Li, M.; Tang, H. X.; Roukes, M. L. *Nat. Nanotechnol.* **2007**, *2* (2), 114−120.
(11) Li, M.; Myers, E. B.; Tang, H. X.; Aldridge, S. J.; McCaig, H. C.; Whiting, J. J.; Simonson, R. J.; Lewis, N. S.; Roukes, M. L. *Nano Lett.* **2010**, *10* (10), 3899−3903.
(12) Ekinci, K. L.; Yang, Y. T.; Roukes, M. L. *J. Appl. Phys.* **2004**, *95* (5), 2682−2689.
(13) Yang, Y. T.; Callegari, C.; Feng, X. L.; Ekinci, K. L.; Roukes, M. L. *Nano Lett.* **2006**, *6* (4), 583−586.
(14) Chiu, H. Y.; Hung, P.; Postma, H. W. C.; Bockrath, M. *Nano Lett.* **2008**, *8* (12), 4342−4346.
(15) Jensen, K.; Kim, K.; Zettl, A. *Nat. Nanotechnol.* **2008**, *3* (9), 533−537.
(16) Chaste, J.; Eichler, A.; Moser, J.; Ceballos, G.; Rurali, R.; Bachtold, A. *Nat. Nanotechnol.* **2012**, *7* (5), 301−304.
(17) Wright, Y. J.; Kar, A. K.; Kim, Y. W.; Scholz, C.; George, M. A. *Sens. Actuators, B* **2005**, *107* (1), 242−251.
(18) Bietsch, A.; Zhang, J. Y.; Hegner, M.; Lang, H. P.; Gerber, C. *Nanotechnology* **2004**, *15* (8), 873−880.
(19) Rühe, J. Polymer Brushes: On the Way to Tailor-Made Surfaces. In *Polymer Brushes*; Wiley-VCH Verlag GmbH & Co. KGaA: Berlin, 2005; pp 1−31.
(20) Matyjaszewski, K.; Xia, J. H. *Chem. Rev.* **2001**, *101* (9), 2921−2990.
(21) Bumbu, G. G.; Wolkenhauer, M.; Kircher, G.; Gutmann, J. S.; Berger, R. *Langmuir* **2007**, *23* (4), 2203−2207.
(22) Abu-Lail, N. I.; Kaholek, M.; LaMattina, B.; Clark, R. L.; Zauscher, S. *Sens. Actuators, B* **2006**, *114* (1), 371−378.
(23) Bradley, C.; Jalili, N.; Nett, S. K.; Chu, L. Q.; Forch, R.; Gutmann, J. S.; Berger, R. *Macromol. Chem. Phys.* **2009**, *210* (16), 1339−1345.
(24) Chen, T.; Chang, D. P.; Liu, T.; Desikan, R.; Datar, R.; Thundat, T.; Berger, R.; Zauscher, S. *J. Mater. Chem.* **2010**, *20* (17), 3391−3395.
(25) Bumbu, G. G.; Kircher, G.; Wolkenhauer, M.; Berger, R.; Gutmann, J. S. *Macromol. Chem. Phys.* **2004**, *205* (13), 1713−1720.
(26) Yang, Y. T.; Ekinci, K. L.; Huang, X. M. H.; Schiavone, L. M.; Roukes, M. L.; Zorman, C. A.; Mehregany, M. *Appl. Phys. Lett.* **2001**, *78* (2), 162−164.
(27) Bargatin, I.; Myers, E. B.; Arlett, J.; Gudlewski, B.; Roukes, M. L. *Appl. Phys. Lett.* **2005**, *86* (13), 3.
(28) Bargatin, I.; Kozinsky, I.; Roukes, M. L. *Appl. Phys. Lett.* **2007**, *90* (9), 3.
(29) Jones, D. M.; Huck, W. T. S. *Adv. Mater.* **2001**, *13* (16), 1256−1259.
(30) Severin, E. J.; Doleman, B. J.; Lewis, N. S. *Anal. Chem.* **2000**, *72* (4), 658−668.
(31) Grate, J. W.; Snow, A.; Ballantine, D. S.; Wohltjen, H.; Abraham, M. H.; McGill, R. A.; Sasson, P. *Anal. Chem.* **1988**, *60* (9), 869−875.
(32) Severin, E. J.; Lewis, N. S. *Anal. Chem.* **2000**, *72* (9), 2008−2015.
(33) Doleman, B. J.; Severin, E. J.; Lewis, N. S. *Proc. Natl. Acad. Sci. U.S.A.* **1998**, *95* (10), 5442−5447.
(34) Bargatin, I.; Myers, E. B.; Aldridge, J. S.; Marcoux, C.; Brianceau, P.; Duraffourg, L.; Colinet, E.; Hentz, S.; Andreucci, P.; Roukes, M. L. *Nano Lett.* **2012**, *12* (3), 1269−1274.
(35) Gupta, A. K.; Nair, P. R.; Akin, D.; Ladisch, M. R.; Broyles, S.; Alam, M. A.; Bashir, R. *Proc. Natl. Acd. Sci. U.S.A.* **2006**, *103* (36), 13362−13367.
(36) Tamayo, J.; Ramos, D.; Mertens, J.; Calleja, M. *Appl. Phys. Lett.* **2006**, *89* (22), 3.
(37) Ramos, D.; Tamayo, J.; Mertens, J.; Calleja, M.; Zaballos, A. *J. Appl. Phys.* **2006**, *100* (10), 3.
(38) Lee, D.; Kim, S.; Jung, N.; Thundat, T.; Jeon, S. *J. Appl. Phys.* **2009**, *106* (2), 024310.
(39) *Poly(methyl methacrylate)*; MSDS No. 037A; Scientific Polymer Products, Inc.: Ontario, NY, Feb 2012.
(40) Berens, A. R.; Hopfenberg, H. B. *J. Membr. Sci.* **1982**, *10*, 283−303.
(41) Sanopoulou, M.; Petropoulos, J. H. *Macromolecules* **2001**, *34* (5), 1400−1410.
(42) Ferrari, M.-C.; Piccinini, E.; Giacinti Baschetti, M.; Doghieri, F.; Sarti, G. C. *Ind. Eng. Chem. Res.* **2008**, *47* (4), 1071−1080.
(43) De Angelis, M. G.; Sarti, G. C. *Annu. Rev. Chem. Biomol. Eng.* **2011**, *2* (1), 97−120.
(44) Guo, J.; Barbari, T. A. *Macromolecules* **2008**, *41* (20), 7762−7764.
(45) Subramanian, S.; Heydweiller, J. C.; Stern, S. A. *J. Polym. Sci., Part B: Polym. Phys.* **1989**, *27* (6), 1209−1220.
(46) *CRC Handbook of Chemistry and Physics*, 82nd ed.; CRC Press: Boca Raton, FL, 2001.